

First measurement of the edge charge exchange recombination spectroscopy on EAST tokamak

Y. Y. Li, X. H. Yin, J. Fu, D. Jiang, S. Y. Feng, B. Lyu, Y. J. Shi, Y. Yi, X. J. Zhou, C. D. Hu, M. Y. Ye, and B. N. Wan

Citation: [Review of Scientific Instruments](#) **87**, 11E501 (2016); doi: 10.1063/1.4955279

View online: <http://dx.doi.org/10.1063/1.4955279>

View Table of Contents: <http://aip.scitation.org/toc/rsi/87/11>

Published by the [American Institute of Physics](#)

Articles you may be interested in

[Electron density profile measurements from hydrogen line intensity ratio method in Versatile Experiment Spherical Torus](#) Contributed paper, published as part of the Proceedings of the 21st Topical Conference on High-Temperature Plasma Diagnostics, Madison, Wisconsin, USA, June 2016.

[Review of Scientific Instruments](#) **87**, 11E54011E540 (2016); 10.1063/1.4960535

[Measurement of helium-like and hydrogen-like argon spectra using double-crystal X-ray spectrometers on EAST](#) Contributed paper, published as part of the Proceedings of the 21st Topical Conference on High-Temperature Plasma Diagnostics, Madison, Wisconsin, USA, June 2016.

[Review of Scientific Instruments](#) **87**, 11E32611E326 (2016); 10.1063/1.4960504

[Upgrades of poloidal and tangential x-ray imaging crystal spectrometers for temperature and rotation measurements on EAST](#) Contributed paper, published as part of the Proceedings of the 21st Topical Conference on High-Temperature Plasma Diagnostics, Madison, Wisconsin, USA, June 2016.

[Review of Scientific Instruments](#) **87**, 11E34211E342 (2016); 10.1063/1.4963150

Applied Physics Reviews

SAVE THE DATE!

3D Bioprinting: Physical and Chemical Processes

May 2–3, 2017 • Winston Salem, NC, USA

First measurement of the edge charge exchange recombination spectroscopy on EAST tokamak

Y. Y. Li,^{1,a)} X. H. Yin,^{1,2} J. Fu,¹ D. Jiang,¹ S. Y. Feng,^{1,2} B. Lyu,¹ Y. J. Shi,^{2,3} Y. Yi,² X. J. Zhou,⁴ C. D. Hu,¹ M. Y. Ye,² and B. N. Wan¹

¹*Institute of Plasma Physics, Chinese Academy of Sciences, Hefei, China*

²*School of Nuclear Science and Technology, University of Science and Technology of China, Hefei, China*

³*Department of Nuclear Engineering, Seoul National University, Seoul 151-742, South Korea*

⁴*Anhui Institute of Optics and Fine Mechanics, Chinese Academy of Sciences, Hefei 230031, China*

(Presented 8 June 2015; received 3 June 2016; accepted 13 June 2016; published online 8 July 2016)

An edge toroidal charge exchange recombination spectroscopy (eCXRS) diagnostic, based on a heating neutral beam injection (NBI), has been deployed recently on the Experimental Advanced Superconducting Tokamak (EAST). The eCXRS, which aims to measure the plasma ion temperature and toroidal rotation velocity in the edge region simultaneously, is a complement to the exiting core CXRS (cCXRS). Two rows with 32 fiber channels each cover a radial range from ~ 2.15 m to ~ 2.32 m with a high spatial resolution of ~ 5 -7 mm. Charge exchange emission of Carbon VI CVI at 529.059 nm induced by the NBI is routinely observed, but can be tuned to any interested wavelength in the spectral range from 400 to 700 nm. Double-slit fiber bundles increase the number of channels, the fibers viewing the same radial position are binned on the CCD detector to improve the signal-to-noise ratio, enabling shorter exposure time down to 5 ms. One channel is connected to a neon lamp, which provides the real-time wavelength calibration on a shot-to-shot basis. In this paper, an overview of the eCXRS diagnostic on EAST is presented and the first results from the 2015 experimental campaign will be shown. Good agreements in ion temperature and toroidal rotation are obtained between the eCXRS and cCXRS systems. *Published by AIP Publishing.* [<http://dx.doi.org/10.1063/1.4955279>]

I. INTRODUCTION

Charge exchange recombination spectroscopy (CXRS) has been extensively utilized to measure the plasma rotation and ion temperature by the Doppler shift and their Doppler broadening of the emission lines in magnetically confined high temperature plasmas.¹⁻³ CXRS on Experimental Advanced Superconducting Tokamak (EAST) monitors routinely the Carbon VI CVI (529.059 nm, $n = 8-7$) spectral line emitted during the interaction of C^{6+} impurity ions with neutrals injected by a heating beam. Each neutral beam injection (NBI)⁴ on EAST has two toroidally separated sources (one, denoted as T-NBI, is more tangential than the other one, P-NBI) and operates at 50-80 kV using deuterium. The nominal width and height for each beam are 0.12 m (horizontal) and 0.48 m (vertical), respectively. The core toroidal CXRS (cCXRS) has been installed successfully and obtained satisfactory experimental results since 2014,⁵ but the radial resolution is too poor (~ 4 cm) at the edge of the plasma to better understand the edge phenomenon such as edge transport barrier, the new edge toroidal CXRS (eCXRS) complements the existing cCXRS.

This paper is organized as follows. Section II introduces the experimental setup of edge CXRS diagnostic, spectro-

scopic hardware as well as the spectrum calibration, Section III presents the preliminary experimental results and then finally, Section IV concludes the paper.

II. EXPERIMENTAL SETUP

The geometry of the first co-NBI⁶ located at the equatorial plane of port A on EAST, the eCXRS collection optics and the sightlines are shown in Fig. 1. The setup consists of telecentric collection optics, a fiber bundle, a high throughput lens-based spectrometer⁷ (2160 grooves per mm, $f = 0.4$ m, $f/\# \sim 2.8$, Bunkoukeiki CLP-400), and a fast-read electron multiplication charge-coupled device (EMCCD). The collection optics, mounted horizontally at the midplane of the horizontal port P, has been aligned to eliminate the poloidal component. The head of the fiber bundle is tilted horizontally at an angle of 1.702° to calibrate the tilt observation plane. The optical head is equipped with 64 silica fibers (diameter of 200 μm , numerical aperture of 0.22) which are divided into two vertically displaced rows. Sightlines in each column view the same spatial position and can be added together to enhance signal level, enabling measurements at a higher temporal resolution. The distance between two rows is 250 μm and equals to the cladding diameter of the fibers. The 32 horizontally evenly distributed observation sightlines are aligned with the center of the T-NBI and cover the plasma edge region ($R = 2.15$ -2.32 m) along the path of the neutral beam. The magnification of the optics is about 20 due to spatial restrictions

Note: Contributed paper, published as part of the Proceedings of the 21st Topical Conference on High-Temperature Plasma Diagnostics, Madison, Wisconsin, USA, June 2016.

^{a)}Author to whom correspondence should be addressed. Electronic mail: liyy@ipp.ac.cn.

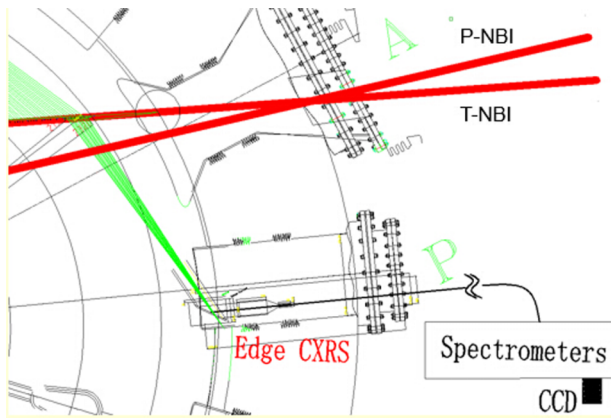


FIG. 1. Schematic layout of the edge CXRS system on EAST.

and the spot size for each fiber image is 4 mm. The spatial resolution is degraded to 5-7 mm by the integration effect toward the EAST center because the sightlines cross many more flux surfaces in the emission region. The distance of two rows at the intersection between the sightlines and the T-NBI is about 5 mm, which is considerably smaller than the size of the heating beam (~ 48 cm).

In the spectrometer side (see Fig. 2), the 64 input fibers are arranged into two vertical columns with 32 channels each at the entrance of the spectrometer to increase the number of channels captured on the CCD simultaneously. An interference filter (highlighted in the red box in Fig. 2) is installed on the camera output lens to avoid the spectra overlapping. Fig. 3 shows the transmission function of the filter measured by using the Photo Research integrating sphere,⁸ where the filter transmission shift due to the slightly off-normal incidence angle, which is different for each channel, is also taken into account. The filter function is fitted with five Gaussians, which facilitates the transmission subtraction from the experimental data. The full width at half maximum (FWHM) of the interference filter is around 2.5 nm, and the peak transmission is about 45% at the peak wavelength of 528.85 nm and it has an out-of-band blocking of $\sim 10^{-3}$.

Wavelength calibration and the instrumental function are obtained for all fiber channels using Ne I lines (527.403 93,

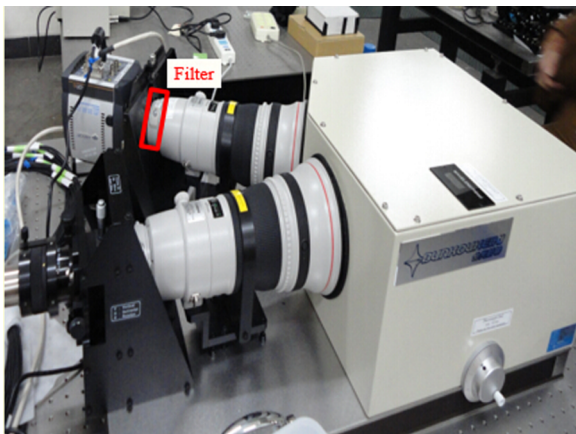


FIG. 2. Photograph of the spectrometer system for the eCXRS system on EAST.

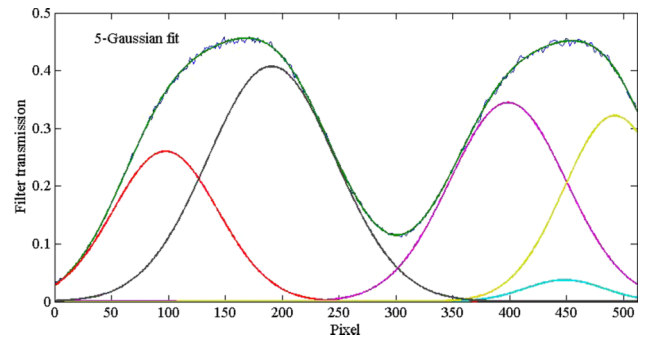


FIG. 3. Interference filter transmission function, which can be fitted with a 5-Gaussian function.

528.008 53, 529.818 91, and 530.4758 nm)⁹ from a neon pencil-type lamp. To increase the number of photons collected, the entrance slit was removed. In this condition, each Ne I line is fitted separately with a multi-Gaussian function depending on the spectral function shape, as shown in Fig. 4. The resultant dispersion is about 0.0116 nm/pixel at 529 nm. Absolute intensity calibration of each channel is performed inside the vessel via an absolutely calibration integrating sphere source.¹⁰ The plane perpendicular to the line-of-sight is determined by a mirror fixed on exit port of the integrating sphere and a backlit laser. The integrating sphere is then positioned, with the mirror and laser removed, the channel is backlit with the integrating sphere. This is repeated for all channels and provides the absolute calibration of the whole system.

An Andor iXon Ultra, back-illuminated, frame-transfer charge coupled device (CCD) camera with on-chip multiplication gain and 512×512 pixels with pixel size of $16 \times 16 \mu\text{m}$ (DU-897U-CS0-#BV) are coupled to the exit of the spectrometer. Hardware vertical binning of 13×256 pixels is used for each channel. With on chip binning of 32 regions of interest, the integration time of this system can reach up to 5 ms.

III. FIRST RESULTS

Edge toroidal rotation is quite small, hence accurate and real-time wavelength calibration becomes more important. One channel is connected to a neon lamp to provide wavelength calibration on a shot-to-shot basis. The image

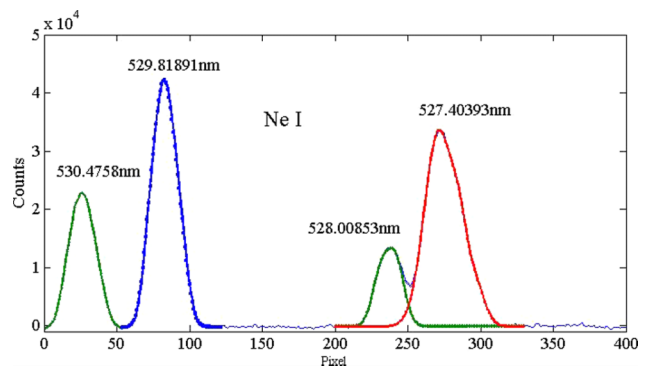


FIG. 4. Spectrum of Ne I lines. Each line is fitted separately using a multi-Gaussian function.

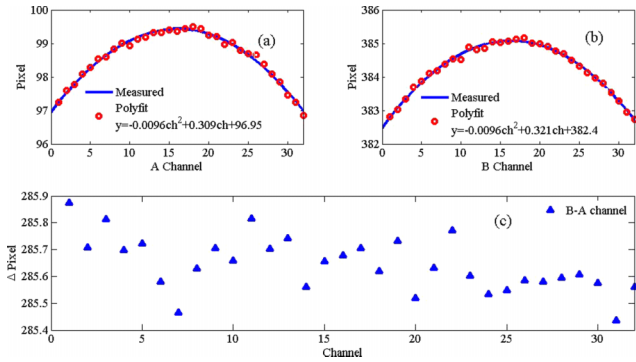


FIG. 5. Wavelength shift curve due to the aberration of the spectrometer.

curvature¹¹ on the CCD detector due to the aberration of the off-axis rays has been determined by using NeI line at 529.8191 nm, as shown in Fig. 5. Those two wavelength shift curves are fitted using a 2nd polynomial fit, respectively. The spectra from the right column channels are shifted by the corresponding pixel difference, as shown in Fig. 5(c), and added to the same spectra of the left channels to improve the signal to noise ratio.

The cross-section contributions¹² to the edge ion temperature and toroidal rotation velocity are estimated by the simulation of spectra (SOS)¹³ and can be negligible. Both the Zeeman effect and fine structure due to the presence of the magnetic field are calculated using simple parametric approximation according to Ref. 14. The true ion temperature is obtained by multiplying the measured apparent temperature with the correction factor. The influence on the rotation is not considered here. A 2-Gaussian fit is used, one accounting for the active line, one for the passive component. The width and shift of the passive spectra during the NBI are fixed to the value of the passive component before NBI in the fit and the amplitude is set to be a free parameter. Here, the change of the passive spectra during the neutral beam injection is not considered.

Fig. 6 shows the first experimental results of the ion temperature and toroidal rotation profiles from the L- and H-mode phases, respectively. The shot number is 54 503 and the integration time is 30 ms. Good consistence between the cCXRS and eCXRS results is observed. Both the edge and core toroidal rotations are observed to increase in the co-current

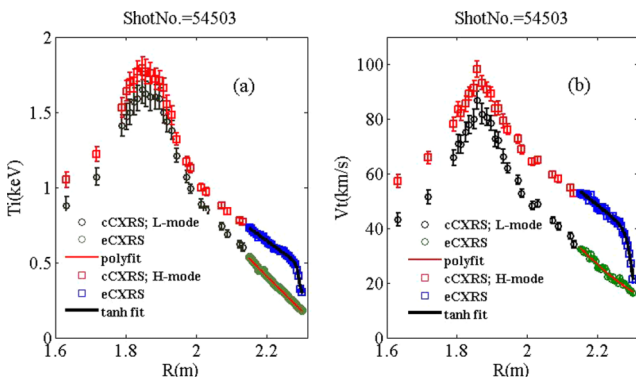


FIG. 6. Ion temperature (a) and toroidal rotation (b) profiles of carbon impurity ions in L- (circle) and H-mode (square) phases in a co-NBI heating discharge.

direction from L-mode to H-mode and the ion temperature increases correspondingly. As illustrated in the figure, in L-mode case, the ion temperature and toroidal rotation change linearly at the plasma edge and can be fitted with a second order polynomial fit, while during the H-mode phase, there is an evident edge pedestal gradient formation both in the profiles of the ion temperature and toroidal rotation. The edge ion temperature and toroidal rotation profiles in H-mode state are well fit to the modified tanh function.¹⁵ The width of the toroidal rotation pedestal (~ 4.4 cm) exceeds that (~ 1.65 cm) of the ion temperature pedestal, consistent with the results from KSTAR H-mode discharges.¹⁶

IV. CONCLUSION

A 32-channel edge toroidal CXRS system has been developed to obtain the edge high spatial resolution ion temperature and toroidal rotation on EAST. Preliminary measurements of edge ion temperature and toroidal rotation were performed in the latest experimental campaign of 2015. The temporal and spatial resolutions can be up to ~ 5 ms and 5-7 mm, respectively. A real-time wavelength calibration is performed to minimize the systematic uncertainties and wavelength change due to the change of air temperature and grating thermal expansion. Good agreements are found between the toroidal core and edge CXRS systems. Carbon impurity density will be obtained combining the CXRS and beam emission spectroscopy (BES) in the near future. Combination of the measurements of the core and edge system allows to obtain the full radial profiles of impurity ion temperature, toroidal rotation velocity and impurity density on EAST.

ACKNOWLEDGMENTS

This work was supported by the National Natural Science Foundation of China (Grant No. 11405212) and the National Magnetic Confinement Fusion Science Program of China (Grant Nos. 2015GB101000, 2015GB103000, and 2013GB112004). The authors would like to thank Dr. Manfred von Hellermann and Dr. Katsumi Ida for their contributions to the development of the CXRS system on EAST.

¹R. C. Isler, *Plasma Phys. Controlled Fusion* **36**, 171 (1994).

²R. J. Fonck *et al.*, *Phys. Rev. A* **29**, 3288 (1984).

³D. M. Thomas *et al.*, *Fusion Sci. Technol.* **53**, 487 (2008), available online at http://www.ans.org/pubs/journals/fst/a_1678.

⁴C. D. Hu *et al.*, *Plasma Sci. Technol.* **17**, 817 (2015).

⁵M. Y. Ye *et al.*, *Fusion Eng. Des.* **96-97**, 1017 (2015).

⁶B. Wu *et al.*, *Fusion Eng. Des.* **86**, 947 (2011).

⁷K. Ida *et al.*, *Rev. Sci. Instrum.* **79**, 053506 (2008).

⁸Photo Research, Inc., 9731 Topanga Canyon Place, Chatsworth, CA 91311-4135, USA.

⁹Y. Ralchenko *et al.*, NIST Atomic Spectra Database (Version 5.0), National Institute of Standards and Technology, Gaithersburg, MD 2015, <http://www.nist.gov/pml/data/asd.cfm>.

¹⁰Y. Zhang *et al.*, *Fusion Eng. Des.* **96-97**, 840 (2015).

¹¹R. E. Bell *et al.*, *Rev. Sci. Instrum.* **70**, 821 (1998).

¹²R. B. Howell *et al.*, *Rev. Sci. Instrum.* **59**, 1521 (1988).

¹³M. G. von Hellermann *et al.*, *Nucl. Instrum. Method A* **623**, 720 (2010), <http://www.rijnhuizen.nl/users/cxrs/mgvh/simuserpackage>, contact address: mgvonhellermann@gmail.com.

¹⁴A. Blom and C. Jupen, *Plasma Phys. Controlled Fusion* **44**, 1229 (2002).

¹⁵J. W. Hughes *et al.*, *Phys. Plasmas* **13**, 056103 (1998).

¹⁶W.-H. Ko *et al.*, *Nucl. Fusion* **55**, 083013 (2015).